A Pseudo-CMOS bootstrap DIGOTA in a 600nm Flexible IGZO Technology

A Pseudo-CMOS bootstrap DIGOTA in a 600nm Flexible IGZO Technology

[1]Diogo Sousa, [1]João Marcelino, [1]Ângelo Santos, [1]Hugo Viana,
[1]João Xavier, [1]Pedro Barquinha, [2]Pedro Toledo, [3]Paolo Crovetti
[1] Nova School of Science and Technology, Lisbon - Portugal
[2]Synopsys, Lisbon - Portugal, [3] Politecnico di Torino, Turin - Italy

***Abstract*—The design of a Digital-Based Operational Transconductance Amplifier (DIGOTA) featuring pseudo-CMOS inverters based on bootstrap pseudo-pMOS devices integrated in a 600 nm Indium-Gallium-Zinc-Oxide (IGZO) Thin-Film Transistors (TFT) Flexible Integrated Circuits (FlexICs) technology is presented in this paper. Based on post-layout simulations, the proposed DIGOTA operates at 3 V power supply and achieves a DC gain of 33.8 dB and a GBW of 64.9 kHz at 221 μW power. Despite maintaining performance comparable to the previous Flexible DIGOTA, this new design occupies 26% less area, requires less logical gates, and enhances the slew rate whilst maintaining reasonable energy efficiency and large signal figures of merit of 14.5 MHz·pF/mW and 50.2 V.pF/s.mW, respectively.**

***Index Terms*—Flexible Integrated Circuits (FlexICs), Operational Transconductance Amplifier (OTA), Digital-Based Circuit, Indium-Gallium-Zinc-Oxide (IGZO), Thin-Film Transistors (TFT), Pseudo-CMOS Bootstrapped Inverter**

I. Introduction

Recently, relevant progress in circuit design is being made with the development of flexible integrated circuits using TFTs [1]. These environmental-friendly circuits are essential for the creation of innovative products that can capitalize on their low fabrication costs [2], high efficiency, and unique physical properties such as flexibility [3], [4] and light transparency. Such unique features, indeed, are paving the way to many applications in the Internet of Things (IoT), in display technology and wearable electronics [5]. In details, flexible electronics has been rapidly emerging as an alternative to conventional silicon chips in areas where the use of inexpensive devices is of paramount importance, giving rise to more complex and useful circuits such as dynamic frequency dividers [6], a flexible 32-bit ARM processor [7], a flexible MOS 6502 microprocessor [8], a hardwired machine learning processing engine [9] and AM receivers [10] that can be integrated into a variety of consumer products and industrial applications.

Contributions to flexible analog building blocks such as Operational Transconductance Amplifiers (OTAs) are still limited in number [11–15] and generally exhibit relatively poor performance due to the intrinsic limitations of IGZO technology and to the lack of complementary devices.

In this context, digital-based analog design techniques [16–20] have gained momentum, leading to the design of a flexible DIGOTA in 800 nm TFT FlexIC technology [21]. While the DIGOTA design presented in [21] is based on nMOS-only logic gates with resistive loads [], this work explores explores an alternative DIGOTA implementation which takes advantage of a pseudo-CMOS logic gates in which a transistor with complementary polarity (pseudo-pMOS) is obtained by bootstrap techniques [22], [23]. The new topology is designed and tested in the 600 nm a-IGZO FlexIC technology provided by Pragmatic.

The rest of this work is structured as follows: Section II describes the proposed circuit and how it works, highlighting the differences from the original design first published in [21]. The results of the post-layout are discussed in section III and subsequently compared with the state-of- the-art, and finally, section IV summarizes the results of the present work.

II. Proposed Design and Circuit Description

The proposed DIGOTA is a single-ended OTA based on the architecture originally introduced in [24] Fig. 1a. In details, it entails a resistive summing network, a cascade of inverters, an output stage and a common-mode extractor, each comprising a NOR logic gate and a three-state digital buffer.

The operation of the circuit is related to the digital outputs OUT+ and OUT- of the cascade of inverters: if OUT+ and OUT- have different binary values (OUT+="1"("0") and OUT-="0"("1")) the output stage is activated and drives the output load. Otherwise, considering OUT+=OUT-, the common-mode extractor feedback circuit its activated: if the logic value is high ($V_{CM} > V_{TP}$), it lowers the V_{CM} node; if the logic value is low ($V_{CM} < V_{TP}$), it increases the V_{CM} node in order to return to one of the first two conditions. A detailed description of the DIGOTA operation is presented in [24],[25].

The first inverters of the cascade are responsible for the conversion from an analog voltage to a digital signal and are particular important for the DIGOTA performance. In the former DIGOTA implementation in IGZO technology [21], nMOS-only resistive inverters have been introduced, which present a low trip point voltage (V_{TP}) and asymmetric rise time [26].

Aiming to address the limitations of nMOS-only resistive gates in IGZO technology, the pseudo-CMOS bootstrap architecture shown in Fig.1a was introduced in [23] to enable a higher trip point, a faster rise time, and rail-to-rail output swing, at the cost of higher power dissipation and area. The faster rise time results in increase and symmetric slew rate and higher DC gain compared with a resistive-load inverter. In consideration of these advantages, pseudo-CMOS inverters are

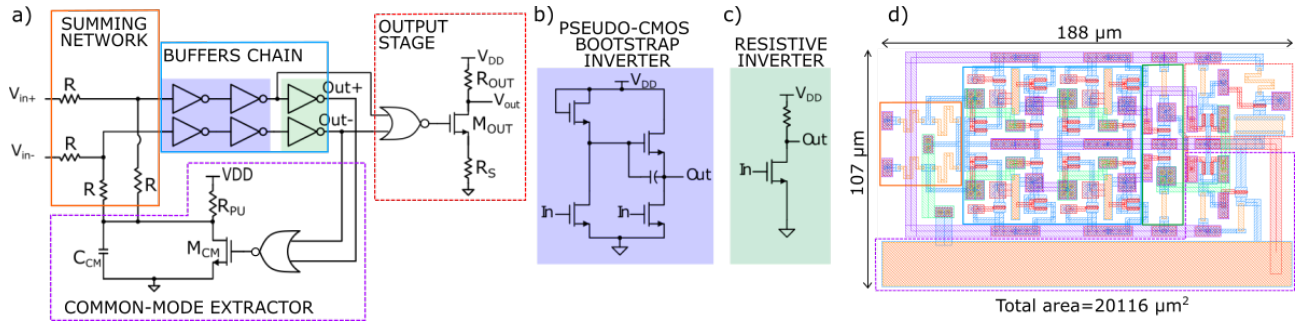

Fig. 1: DIGOTA schematic(a), pseudo-CMOS bootstrap inverter's schematic (b), resistive inverter's schematic (c), DIGOTA layout (d).

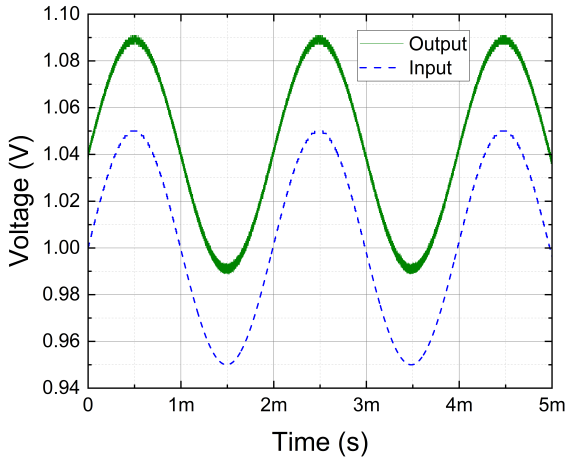

Fig. 2: Post-layout transient simulated input and output wave in voltage-follower configuration.

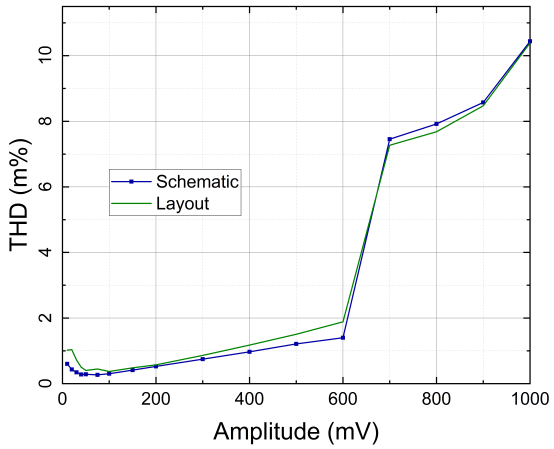

Fig. 4: THD (m%) versus input amplitude.

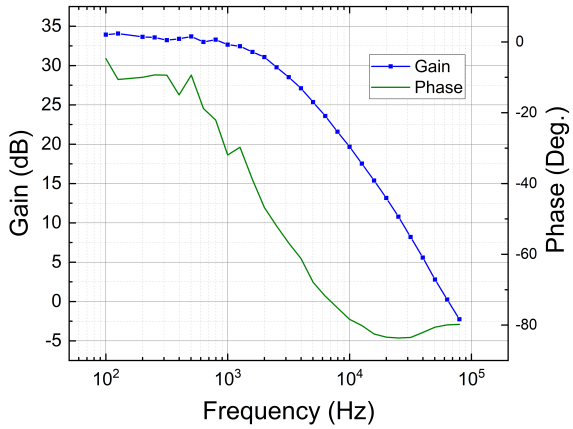

Fig. 3: Simulated frequency response.

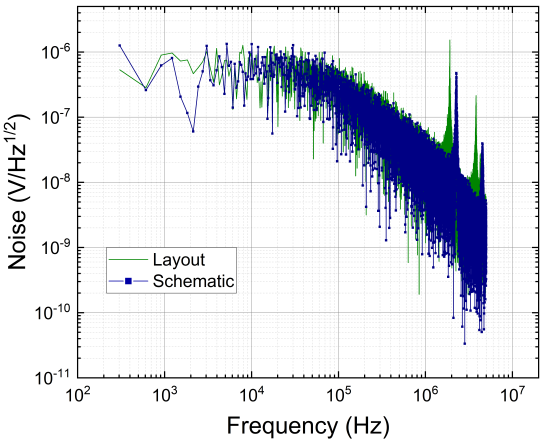

Fig. 5: Noise power spectral density.

introduced in the first stages of the buffer chain of the DIGOTA design proposed in this work, taking into advantage the higher common mode input rage offered by this architecture.

III. Simulation Results

The Pseudo-CMOS DIGOTA describeb in II has been designed for fabrication in the PragmatIC 600 nm IGZO TFT technology and its layout is shown in Fig. 1 (b). The DIGOTA performance have been assessed based on post-layout simulations in the voltage follower configuration, with a supply voltage (V_{DD}) of 3 V, and a load of 50 pF in parallel with 4 M. Corner analysis has been performed to assess the impact of a 10% variation in V_{DD}, encompassing a range of transistor variations (fast, typical, and slow) and resistance values (maximum, nominal, and minimum).

The response to a sinewave input at 50 mV peak amplitude and 500 Hz frequency is presented in Fig. 2. The output presents the characteristic ripple observed in all DIGOTAs. The frequency response of the amplifier is presented in Fig. 3. Due to its dynamic operation, this analysis was conducted by

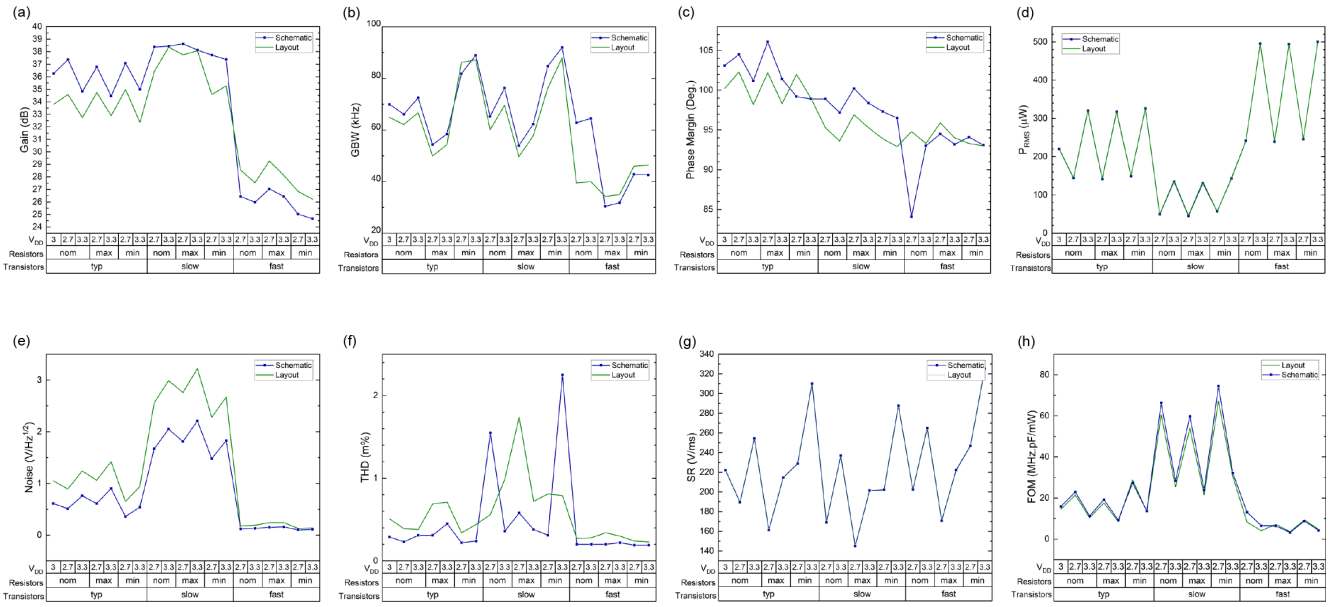

Fig. 6: PivotCharts of schematic and post-layout simulation results for (a) DC gain, (b) gain band width (GBW), (c) phase margin (PM), , (d) power dissipation, (e) in-band noise, (f) THD, (g) slew rate (SR) and (h) figure of merit (FoM).

sweeping the input wave frequency in a transient simulation. It is possible to observe that the circuit behaves as a single pole system, with the pole located at around 2 kHz. has a DC gain of 33.8 dB, a gain-bandwidth product (GBW) of 65 kHz, and a phase margin of 100°.

Considering a noise bandwidth close to 100×GBW, i.e. 10 GHz, Fig. 5 reveals an in-band noise of 1.05 mV_{rms}. The Total Harmonic Distortion (THD) analysis presented in Fig. 4 aims to evaluate the impact of input amplitude on the output distortion. The THD value is as low as 0.40 % at 50 mV amplitude and less than 10.4% up to 1 V peak amplitude.

The circuit's performance between schematic-only and post-layout simulation results across process-voltage (PV) corners, pivot charts are presented in Fig. 6.

Post-layout simulations reveal a nominal value of DC gain of 33.8 dB and a worst case of 26.2 dB while demonstrating the tendency of lowering the DC gain for fast transistors corners, as can be seen in Fig. 6 (a).

Regarding GBW results, presented in Fig. 6 (b), it is possible to conclude that this parameter is one of the most sensitive to PV since it varies from 65 kHz in the nominal corner, with the worst corner lowering it to 35 kHz. Once more, it is possible to notice that the maximum resistance corners present a generally lower GBW due to the increasing output impedance that leads to a lower frequency of the dominant pole.

On the other hand the PM is very insensitive to corners variation and is always above 84°, as shown in Fig 6 (c), which corresponds to a robustly stable closed-loop operation across corners, as expected for a single-pole circuit.

From Fig. 6 (d), power consumption is strongly correlated with the transistor's process corner. The pre-layout analysis yielded a value of 220 μW for the nominal case, and 500 μW for the worst case. Notably, the inclusion of parasitic elements did not significantly alter these values, with post-layout results indicating an almost identical consumption of 221 μW for the nominal condition and 500 μW for the worst-case corner.

Fig. 6 (e) presents the pivot-chart for in-band noise. It is possible to see that the value for the nominal corner is 1.05 mV_{rms} and for the worst corner is 2.99 mV_{rms}.

The THD parameter was also tested across corners for an input amplitude value of 50 mV and 500 Hz of input frequency and the results are presented in Fig. 6 (f). Regarding post-layout values, despite the worst corner presenting a value of 1.74%, the remaining corners present a lower THD, including the nominal value, with a value of 0.51 %.

From Fig. 6 (g) it is observed that parasitics have almost no influence on the slew rate. The nominal value changed from 221.9 kV/s to 221.6 kV/s and the worst case value from 145.1 kV/s to 144.8 kV/s.

The energy efficiency figure of merit (FoM), defined as $(\text{GBW}\cdot C_{\text{out}})/\text{Power}$, across PV variation is shown in Fig.6 (h). For post-layout, the obtained values were 14.5 MHz.pF/mW and 3.55 MHz.pF/mW for nominal and worst corner, respectively.

Table I presents the comparison between existing literature and the proposed topology for typical and worst PV corner. The proposed DIGOTA operates at the lowest supply voltage and achieves the highest slew rate, while occupying the smallest area among the other layouts under consideration. Despite the power consumption is about 2× compared to [21] at comparable GBW, but it is competitive with all the other works. A significant benefit of the selected inverter topology is its superior slew rate.

As mentioned in section 2, the gain is highly connected with the reduced number of inverters in the inverter chain. Although the DC gain is not the highest among all the presented in Table I it could be increased just by increasing the number

TABLE I: Comparison of DIGOTA results with the State-of-the-Art among Flexible Operational Transconductance Amplifiers.

	[27]$^{+}$	[28]$^{+}$	[29]$^{+}$	[30]$^{+}$	[21]*	This work*	
						Typical	Worst corner
Technology (Lmin [μm])	a-IGZO (3)	a-IGZO	Flexible IGZO (0.8)	a-IGZO	Flexible IGZO (0.8)	Flexible IGZO (0.6)	
Topology	Analog // Pseudo-CMOS	Analog // Positive feedback	Analog // Common source	Analog // Pseudo-CMOS	Digital based // Resistive	Digital based // Pseudo-CMOS	
DC gain [V]	**57**	32.67	28.9	22.5	36.3	33.8	26.2
GBW [Hz]	311 k	200 k	**3.34 M**	31 k	86 k	64.9 k	34.29 k
Output Load	-	-	50 fF // 1.25 M	15 pF // 1 M	50 pF // 8 M	50 pF // 4 M	
PM [degrees]	75	35.8	-	-	87	**100.2**	92.9
V_{DD} [V]	10	15	8	5	3.3	3	
Consumption [mW]	2.43	0.68	14.2	0.160	**0.113**	0.221	0.500
Area [mm^2]	3.69	4.42	0.33	9.83	0.0252	**0.020**	
Noise [mV_{rms}]	-	-	-	-	**0.087**	1.05	2.99
Slew Rate [V/ms]	-	-	-	-	187	**222**	145
**FoM [MHz.pF/mW]	-	-	11.73	2.91	**38.05**	14.49	3.55

$^{+}$experimental; *simulation, MC mean value; **FOM = $\frac{\text{GBW}\cdot C_{\text{out}}}{\text{Power}}$; **best performance in bold**;

of inverters at the cost of higher power dissipation and larger area.

In spite of such improvements, it can be concluded that, while the introduction of pseudo-CMOS solutions and bootstrapped stages result in a significant gain and performance improvement in traditional analog OTAs in IGZO technologies, the performance of DIGOTAs in Flexible IGZO are only slightly affected in consideration of the digital operation its inherent insensitivity to the analog characteristics of the devices.

IV. Conclusion

This paper presented a Digital-Based (OTA) in a 600 nm IGZO TFT FlexICs technology and exhibited post-layout simulation results comparing them with state-of-the-art literature. The proposed DIGOTA explored a new topology by implementing pseudo-CMOS bootstrap inverters. This modification allowed to achieve a DC gain of 33.8 dB and a GBW of 64.9 kHz, which is in line with the previous DIGOTA, but with less area and fewer gates. The proposed topology also improved the slew rate and the phase margin.

Acknowledgment

The authors acknowledge the support of PragmatIC for providing the technology PDK. This work was financed by (...).

References

1 Bi, S., Gao, B., Han, X., He, Z., Metts, J., Jiang, C., and Asare-Yeboah, K., "Recent progress in printing flexible electronics: A review," *Science China Technological Sciences*, Jul. 2023.

2 Hwan Hwang, Y., Seo, J.-S., Moon Yun, J., Park, H., Yang, S., Ko Park, S.-H., and Bae, B.-S., "An 'aqueous route' for the fabrication of low-temperature-processable oxide flexible transparent thin-film transistors on plastic substrates," *NPG Asia Materials*, vol. 5, no. 4, pp. e45–e45, Apr. 2013, publisher: Nature Publishing Group.

3 Shabanpour, R., Meister, T., Ishida, K., Boroujeni, B., Carta, C., Ellinger, F., Petti, L., Munzenrieder, N., Salvatore, G., and Troster, G., "A transistor model for a-IGZO TFT circuit design built upon the RPI-aTFT model," in *2017 15th IEEE International New Circuits and Systems Conference (NEWCAS)*. Strasbourg, France: IEEE, Jun. 2017, pp. 129–132.

4 Karnaushenko, D., Münzenrieder, N., Karnaushenko, D. D., Koch, B., Meyer, A. K., Baunack, S., Petti, L., Tröster, G., Makarov, D., and Schmidt, O. G., "Biomimetic Microelectronics for Regenerative Neuronal Cuff Implants," *Advanced Materials*, vol. 27, no. 43, pp. 6797–6805, 2015, _eprint: https://onlinelibrary.wiley.com/doi/pdf/10.1002/adma.201503696.

5 Mirshojaeian Hosseini, M. J. and Nawrocki, R. A., "A Review of the Progress of Thin-Film Transistors and Their Technologies for Flexible Electronics," *Micromachines*, vol. 12, no. 6, p. 655, Jun. 2021, number: 6 Publisher: Multidisciplinary Digital Publishing Institute.

6 Meister, T., Ishida, K., Sou, A., Carta, C., and Ellinger, F., "3.93-MHz/328- μ W Dynamic Frequency Divider in Flexible a-IGZO TFT Technology," *IEEE Solid-State Circuits Letters*, vol. 3, pp. 134–137, 2020.

7 Biggs, J. and *et al.*, "A natively flexible 32-bit Arm microprocessor," *Nature*, vol. 595, no. 7868, pp. 532–536, Jul 2021.

8 Çeliker, H. and *et al.*, "Flex6502: A Flexible 8b Microprocessor in 0.8μm Metal-Oxide Thin-Film Transistor Technology Implemented with a Complete Digital Design Flow Running Complex Assembly Code," in *ISSCC*, vol. 65, 2022, pp. 272–274.

9 Ozer, E. and *et al.*, "A hardwired machine learning processing engine fabricated with submicron metal-oxide thin-film transistors on a flexible substrate," *Nature Electronics*, vol. 3, no. 7, pp. 419–425, Jul 2020.

10 Ishida, K., Shabanpour, R., Meister, T., Boroujeni, B. K., Carta, C., Petti, L., Munzenrieder, N., Salvatore, G. A., Troster, G., and Ellinger, F., "15 dB Conversion gain, 20 MHz carrier frequency AM receiver in flexible a-IGZO TFT technology with textile antennas," in *2015 Symposium on VLSI Circuits (VLSI Circuits)*. Kyoto, Japan: IEEE, Jun. 2015, pp. C194–C195.

11 Shabanpour and *et al.*, "A 70^{o} phase margin OPAMP with positive feedback in flexible a-IGZO TFT technology," in *MWSCAS*, 2015.

12 Tarn, Y.-C. and *et al.*, "An Amorphous-Silicon Operational Amplifier and Its Application to a 4-Bit Digital-to-Analog Converter," *JSSC*, vol. 45, no. 5, pp. 1028–1035, 2010.

13 Dandekar, M., Myny, K., and Dehaene, W., "Positive-Feedback-Based Design Technique for Inherently Stable Active Load Toward High-Gain Amplifiers With Unipolar a-IGZO TFT Devices," *IEEE Solid-State Circuits Letters*, vol. 5, pp. 37–40, 2022.

14 ——, "An a-IGZO TFT based Op-Amp with 57 dB DC-Gain, 311 KHz Unity-gain Freq., 75 deg. Phase Margin and 2.43 mW Power on Flexible Substrate," in *ESSCIRC*, 2021, pp. 407–410.

15 Zulqarnain, M. and Cantatore, E., "Analog and Mixed Signal Circuit Design Techniques in Flexible Unipolar a-IGZO TFT Technology: Challenges and Recent Trends," *IEEE Open Journal of Circuits and Systems*, vol. 2, pp. 743–756, 2021.

16 Alioto, M., *Enabling the Internet of Things – from Integrated Circuits to Integrated Systems*, 1st ed. Springer, 2017.

17 Crovetti, P. S., "A Digital-Based Analog Differential Circuit," *IEEE Trans. Circuits Syst. I: Reg. Papers*, vol. 60, no. 12, pp. 3107–3116, Dec 2013.

18 Toledo, P., Crovetti, P., Aiello, O., and Alioto, M., "Design of digital otas with operation down to 0.3 v and nw power for direct harvesting," *IEEE Transactions on Circuits and Systems I: Regular Papers*, vol. 68, no. 9, pp. 3693–3706, 2021.

19 Toledo, P. and *et al.*, "Fully Digital Rail-to-Rail OTA With Sub-1000-μm^2

Area, 250-mV Minimum Supply, and nW Power at 150-pF Load in 180 nm," *IEEE Solid-State Circuits Letters*, vol. 3, pp. 474–477, 2020.

20 ——, "Design of Digital OTAs With Operation Down to 0.3 V and nW Power for Direct Harvesting," *TCAS-I*, vol. 68, no. 9, pp. 3693–3706, 2021.

21 Adibi, S., Rubino, R., Toledo, P., and Crovetti, P., "Design of an Analog and of a Digital-Based OTA in Flexible Integrated Circuit Technology," in *2022 29th IEEE International Conference on Electronics, Circuits and Systems (ICECS)*. Glasgow, United Kingdom: IEEE, Oct. 2022, pp. 1–4.

22 Tsung-Ching Huang, Fukuda, K., Chun-Ming Lo, Yung-Hui Yeh, Sekitani, T., Someya, T., and Kwang-Ting Cheng, "Pseudo-CMOS: A novel design style for flexible electronics," in *2010 Design, Automation & Test in Europe Conference & Exhibition (DATE 2010)*. Dresden: IEEE, Mar. 2010, pp. 154–159.

23 Bahubalindruni, P. G., Tiwari, B., Pereira, M., Santa, A., Martins, J., Rovisco, A., Tavares, V., Martins, R., Fortunato, E., and Barquinha, P., "Rail-to-Rail Timing Signals Generation Using InGaZnO TFTs For Flexible X-Ray Detector," *IEEE Journal of the Electron Devices Society*, vol. 8, pp. 157–162, 2020.

24 Crovetti, P. S., "A Digital-Based Analog Differential Circuit," *IEEE Transactions on Circuits and Systems I: Regular Papers*, vol. 60, no. 12, pp. 3107–3116, Dec. 2013.

25 Toledo, P., Crovetti, P., Aiello, O., and Alioto, M., "Design of digital otas with operation down to 0.3 v and nw power for direct harvesting," *IEEE Transactions on Circuits and Systems I: Regular Papers*, vol. 68, no. 9, pp. 3693–3706, Sep. 2021.

26 Çeliker, H., Roose, F. D., Willegems, M., Smout, S., Dehaene, W., and Myny, K., "Analysis and comparison of logic architectures for digital circuits in a-igzo thin-film transistor technologies," *IEEE Journal of Solid-State Circuits*, pp. 1–13, 2023.

27 Dandekar, M., Myny, K., and Dehaene, W., "An a-igzo tft based op-amp with 57 db dc-gain, 311 khz unity-gain freq., 75 deg. phase margin and 2.43 mw power on flexible substrate," 2021-01-01.

28 Meng, F., Li, Y., Li, J., Liang, J., and Zhang, J., "A performance optimized operational amplifier using transconductance enhancement topology based on a-igzo tfts," *IEEE Journal of the Electron Devices Society*, vol. PP, pp. 1–1, 01 2024.

29 Meister, T., Ishida, K., Sou, A., Carta, C., and Ellinger, F., "49.35 mhz gbw and 33.43 mhz gbw amplifiers in flexible a-igzo tft technology," *Electronics Letters*, vol. 56, 07 2020.

30 Ishida, K., Shabanpour, R., Boroujeni, B., Meister, T., Carta, C., Ellinger, F., Petti, L., Münzenrieder, N., Salvatore, G. A., and Tröster, G., "22.5 db open-loop gain, 31 khz gbw pseudo-cmos based operational amplifier with a-igzo tfts on a flexible film," *Proceedings - 2014 IEEE Asian Solid-State Circuits Conference, A-SSCC 2014*, pp. 313–316, 01 2015.